



Exploring circumstellar effects on the Li abundances in massive Galactic AGB stars

V. Pérez-Mesa^{1,2}, O. Zamora^{1,2}, D. A. García-Hernández^{1,2}, B. Plez³,
A. Manchado^{1,2,4}, A. I. Karakas⁵, and M. Lugaro^{5,6}

- ¹ Instituto de Astrofísica de Canarias (IAC), E-38205 La Laguna, Tenerife, Spain
e-mail: vperezme@iac
- ² Departamento de Astrofísica, Universidad de La Laguna (ULL), E-38206 La Laguna, Tenerife, Spain
- ³ Laboratoire Univers et Particules de Montpellier, Université de Montpellier2, CNRS, 34095 Montpellier, France
- ⁴ Consejo Superior de Investigaciones Científicas (CSIC), E-28006 Madrid, Spain
- ⁵ Monash Centre for Astrophysics, School of Physics and Astronomy, Monash University, VIC3800, Australia
- ⁶ Konkoly Observatory, Research Centre for Astronomy and Earth Sciences, Hungarian Academy of Sciences, 1121 Budapest, Hungary

Abstract. We have explored the circumstellar effects on the Li abundance determination in a complete sample of O-rich Galactic asymptotic giant branch (AGB) stars, previously studied with hydrostatic models. We use a modified version of the spectral synthesis code Turbospectrum and more realistic extended model atmospheres that consider the presence of a gaseous circumstellar envelope and a radial wind in these massive AGB stars. The Li abundances are determined from the 6708 Å Li I resonance line. The Li pseudo-dynamical abundances obtained are practically identical to those derived with hydrostatic models (a maximum difference of 0.3 dex is found in the only super Li-rich AGB star in our sample). The low Li abundance and therefore negligible Li I column-density in the circumstellar envelope likely explains the small differences between extended and hydrostatic models. Our results confirm the activation of the hot bottom burning (HBB) process in massive Galactic AGB stars.

Key words. stars: AGB and post-AGB – stars: abundances – stars: evolution – nuclear reactions, nucleosynthesis, abundances – stars: atmospheres – stars: late-type

1. Introduction

Stars with initial masses in the range between 0.8 and 8 M_{\odot} end their lives with a phase of strong mass loss and thermal pulses (TP) on the asymptotic giant branch (AGB, Herwig 2005). The AGB stars are one of the main contributors to the chemical enrichment (e.g.

C, N, Li, F, and *s*-elements) of the interstellar medium. The theoretical nucleosynthesis models predict the presence of *s*-elements (such as Rb, Sr, Y, Zr, Ba, La, Nd, Tc, etc.) that can be formed by *slow*-neutron captures (*s*-process) and are dredged up to the stellar surface (García-Hernández et al., 2013). The $^{13}\text{C}(\alpha, n)^{16}\text{O}$ reaction releases neutrons, which

are captured by iron nuclei and other heavy elements, forming *s*-elements that can later be dredge up to the stellar surface in the next thermal pulse (Straniero et al., 1995, 1997; Busso et al., 2001). The $^{13}\text{C}(\alpha, n)^{16}\text{O}$ reaction is the preferred neutron source for $\sim 1\text{-}3 M_{\odot}$.

Another neutron source, $^{22}\text{Ne}(\alpha, n)^{25}\text{Mg}$ takes place during the convective TPs (Straniero et al., 1995, 2000; García-Hernández et al., 2007). The $^{22}\text{Ne}(\alpha, n)^{25}\text{Mg}$ neutron source requires higher temperatures and higher neutron densities than the $^{13}\text{C}(\alpha, n)^{16}\text{O}$ reaction. Thus, a different *s*-element pattern is expected depending on the dominant neutron source. The $^{13}\text{C}(\alpha, n)^{16}\text{O}$ reaction operates during the interpulse period and is the preferred neutron source for masses around $1\text{-}3 M_{\odot}$, while the $^{22}\text{Ne}(\alpha, n)^{25}\text{Mg}$ reaction operates during the convective TP and, in the more massive AGB stars ($\gtrsim 3\text{-}4 M_{\odot}$), the *s*-process elements are formed mainly via the $^{22}\text{Ne}(\alpha, n)^{25}\text{Mg}$ reaction (García-Hernández et al., 2013).

In Pérez-Mesa et al. (2017) are reported new Rb and Zr abundances in a full sample of massive AGB stars, previously studied with hydrostatic models, by using more realistic extended model atmospheres, in which we consider the presence of a circumstellar envelope and radial wind. For this, we used a modified version of the spectral synthesis code Turbospectrum (Plez, 2012; Zamora et al., 2014). The derived Rb abundances were much lower than those obtained with the hydrostatic models, while the Zr abundances were similar. So, we confirmed that the use of extended atmosphere models can resolve the discrepancy between the AGB nucleosynthesis theoretical models and the observations of Galactic massive AGB stars (Pérez-Mesa et al., 2017). Now, we have explored the effects on the Li abundances by considering the presence of a gaseous envelope with and a radial wind in massive AGB stars.

2. Observational data and models

We have used high-resolution optical echelle spectra ($R \sim 50,000$) for the sample of massive Galactic AGB stars by García-Hernández et al.

(2006, 2007). In addition, we have analysed the spectra of the super Li-rich AGBs reported by García-Hernández et al. (2013). By using new extended model atmospheres developed by us (Zamora et al., 2014; Pérez-Mesa et al., 2017), we could obtain the Li abundances (from the 6708 \AA Li I line) in the sample stars. The atmospheric parameters and Li abundances derived with these extended models are listed in Table 1.

3. Results

The new Li abundances derived from our extended models are practically identical (typically within 0.1 dex) to those obtained with the hydrostatic ones (see Table 1). A maximum difference (between the hydrostatic and pseudo-dynamical values) of 0.3 dex is found in the only super Li-rich star (R Cen) in our AGB sample, indicating that the Li content in these stars is only slightly affected by the presence of a circumstellar envelope. Therefore, the conclusions by García-Hernández et al. (2007, 2013) regarding the Li-rich and super Li-rich characters of massive AGB stars at advanced evolutionary stages and at the beginning of the thermally pulsing phase, respectively, remain unchanged. Figure 1 displays examples of the observed spectra and the best synthetic fits from hydrostatic and extended models in the spectral region around Li I 6708 \AA . Both hydrostatic and extended models fit well the observed spectra (both the Li I spectral profile and the wealth of TiO molecular lines) but in few cases, curiously the coolest stars with β values of 1.6 (see Table 1), the depth of the TiO bands is best fitted with extended models around 100 K warmer than the hydrostatic ones.

Our Li results in these stars are at odds with the Rb ones (from the Rb I 7800 \AA lines; Zamora et al., 2014; Pérez-Mesa et al., 2017); the Rb abundances obtained with extended models are much lower (sometimes even by 1-2 dex) than the hydrostatic ones, being strongly affected by the circumstellar envelope. We have made several tests by changing the wind parameters (mass loss, β and terminal velocity) in the models; e.g., by assuming the wind

Table 1. Atmospheric parameters and Li abundances derived using hydrostatic and extended models. The asterisks indicate that the T_{eff} in the pseudo-dynamic case is 100 K higher than the hydrostatic case.

IRAS name	T_{eff} (K)	β	\dot{M} ($M_{\odot}\text{yr}^{-1}$)	v_{exp} (kms^{-1})	P(days)	$\log\epsilon(\text{Li})_{static}$	$\log\epsilon(\text{Li})_{dyn}$
01085+3022	3300	0.2	1.0×10^{-9}	13	560	2.4	2.3
05027-2158	2800*	1.6	5.0×10^{-7}	8	368	1.1	0.9
05098-6422	3000	0.2	5.0×10^{-7}	6	394	≤ -1.0	≤ 0.0
06300+6058	3000	0.4	5.0×10^{-7}	12	440	0.7	0.7
07304-2032	2700	0.2	1.0×10^{-9}	7	509	0.9	1.0
09429-2148	3300	1.6	1.0×10^{-8}	12	650	2.2	2.2
10261-5055	3000	0.2	1.0×10^{-9}	4	317	≤ -1.0	≤ 0.0
15193+3132	2800	0.2	1.0×10^{-9}	3	360	≤ 0.0	≤ 0.2
15211-4254	3300	1.6	1.0×10^{-9}	11	...	2.3	2.3
15576-1212	3000	0.2	5.0×10^{-7}	10	415	1.1	1.1
16030-5156	3000	1.6	5.0×10^{-8}	10	579	1.5	1.4
16037+4218	2900	0.2	1.0×10^{-9}	4	360	≤ -1.0	≤ 0.0
16260+3454	3300	0.2	1.0×10^{-9}	12	475	2.7	2.6
17034-1024	3300	1.2	1.0×10^{-9}	8	346	≤ 0.0	0.0
18429-1721	3000*	1.6	1.0×10^{-7}	7	481	1.2	0.9
19361-1658	3000	0.2	1.0×10^{-9}	8	...	1.9	2.0
20052+0554	3300	1.6	1.0×10^{-9}	16	450	2.6	2.4
20343-3020	3000	0.2	1.0×10^{-9}	8	349	≤ -1.0	≤ 0.0
R Cen	3000*	1.6	1.0×10^{-9}	5	251	4.3	4.0
RU Cyg	3000	1.6	1.0×10^{-9}	12	442	2.0	1.9

parameters from the best fits of the Rb I 7800 Å line (Pérez-Mesa et al., 2017), but the Li abundances remain very similar (within 0.1 dex). Thus, our conclusion of small circumstellar effects in the derivation of the Li abundances in O-rich AGB stars seems to be solid.

The Li result could be somehow surprising because the atomic parameters (e.g., excitation potential) of the Li I 6708 Å and Rb I 7800 Å resonance lines are quite similar. The low Li abundance and therefore negligible Li I column-density in the circumstellar envelope, however, likely explains the small differences between extended and hydrostatic models.

Finally, the Li-rich stars and super Li-rich character of the massive AGB stars in our sample confirm that they experience strong HBB (García-Hernández et al., 2007, 2013).

This is in good agreement with the predictions from the most recent AGB nucleosynthesis models like the ATON (Di Criscienzo et al., 2016), Monash (Karakas & Lugaro, 2016) and Nugrid/MESA (Pignatari et al., 2016) models but in strong contrast with the FRUITY AGB models (Cristallo et al., 2011, 2015) which do not predict strong HBB in solar metallicity massive AGB stars.

Acknowledgements. V.P.M. acknowledges the financial support from the Spanish Ministry of Economy and Competitiveness (MINECO) under the 2011 Severo Ochoa Program MINECO SEV-2011-0187. V.P.M., O.Z., D.A.G.H. and A.M. acknowledge support provided by the MINECO under grant AYA-2014-58082-P. M.L. is a Momentum (“Lendület-2014” Programme) project leader of the Hungarian Academy of Sciences. This pa-

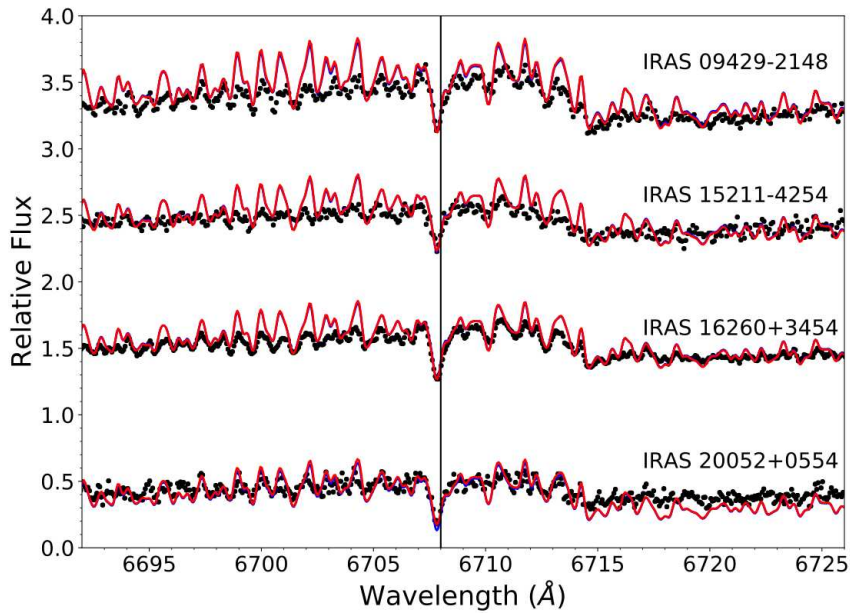


Fig. 1. The Li I 6708 Å spectral regions in massive Galactic AGB stars. The hydrostatic (blue lines) and pseudo-dynamical (red lines) models that best fit the observations (black dots) are shown in four sample stars. The location of the Li I line is indicated by the black vertical line.

per made use of the IAC Supercomputing facility HTCCondor (<http://research.cs.wisc.edu/htcondor/>), partly financed by the Ministry of Economy and Competitiveness with FEDER funds, code IACA13-3E-2493.

References

- Busso, M., et al. 2001, *ApJ*, 557, 802
 Cristallo, S., et al. 2011, *ApJS*, 197, 17
 Cristallo, S., et al. 2015, *ApJS*, 219, 40
 Di Criscienzo, M., et al. 2016, *MNRAS*, 462, 395
 García-Hernández, D. A., et al. 2006, *Science*, 314, 1751
 García-Hernández, D. A., et al. 2007, *A&A*, 462, 711
 García-Hernández, D. A., et al. 2013, *A&A*, 555, L3
 Herwig, F. 2005, *ARA&A*, 43, 435
 Karakas, A. I., & Lugaro, M. 2016, *ApJ*, 825, 26
 Pérez-Mesa, V., Zamora, O., García-Hernández, D. A., et al. 2017, *A&A*, 606, A20
 Plez, B. 2012, *Turbospectrum: Code for spectral synthesis*, Astrophysics Source Code Library 1205.004
 Pignatari, M., et al. 2016, *ApJS*, 225, 24
 Straniero, O., et al. 1995, *ApJ*, 440, L85
 Straniero, O., et al. 1997, *ApJ*, 478, 332
 Straniero, O., et al. 2000, *MmSAI*, 71, 719
 Zamora, O., et al. 2014, *A&A*, 564, L4